

Rotational Branching Ratios in N_2^+ : Observation of Photon Energy Dependence by Photoelectron Spectroscopy

G. Öhrwall,¹ P. Baltzer,¹ and J. Bozek²

¹*Department of Physics, Uppsala University, Box 530, S-751 21 Uppsala, Sweden*

²*Lawrence Berkeley National Laboratory, University of California, Berkeley, California 94720*
(Received 23 February 1998)

Rotational line profiles have been studied as a function of photon energy by use of photoelectron spectroscopy. The relative squared multipole moment matrix elements of the $X^1\Sigma_g^+(\nu=0) \rightarrow X^2\Sigma_g^+(\nu=0)$ transition of N_2 have been determined from the relative intensities of rotational branches for photon energies between 23 and 65 eV. The relative intensities, and hence the multipole moment matrix elements of the rotational branches, are clearly dependent on photon energy. This non-Franck-Condon-like behavior can be explained by a shape resonance in the $3\sigma_g \rightarrow k\sigma_u$ ionization channel. [S0031-9007(98)06637-X]

PACS numbers: 33.60.Cv, 33.70.Jg

Even in the early days of photoelectron spectroscopy, considerable interest was directed towards the influence of rotations on photoelectron spectra of molecules [1,2]. The influence of photon energy on the rotational structure could then be investigated only by using different types of resonance lamps [3]. The extremely small rotational spacing made the use of broadband synchrotron radiation unsuited for rotationally resolved photoelectron spectroscopy. Recent developments in synchrotron radiation technology, notably high-brilliance third-generation facilities and new ultrahigh-resolution monochromators [4–6], as well as advances in photoelectron spectrometer design [7,8] have enabled synchrotron radiation photoelectron studies with rotational resolution. Baltzer *et al.* [9] have earlier presented rotationally resolved spectra of the $\nu=0$ vibration of the X and B states of N_2^+ , recorded with unpolarized light from a He resonance lamp. We have recorded high-resolution photoelectron spectra of the same peaks with synchrotron radiation from the Advanced Light Source (ALS) in Berkeley, California, varying the photon energy between 23 and 65 eV. Results on the $X^2\Sigma_g^+$ state are presented in the present paper. One should also note that the rotational line profiles of the X , A , and B states of N_2^+ were estimated by Allen and Grimm using a deconvolution technique [10]. Morioka *et al.* [11] and Ogata *et al.* [12] investigated the X state in a similar way, but their resolution was inferior to that of Allen and Grimm. In all these cases, the energy resolution was inferior to that of Ref. [9].

With the ZEKE-PFI technique, several rotationally resolved studies of the X state of N_2^+ have been made, both extreme ultraviolet laser excited [13–15] and synchrotron radiation excited [16]. These threshold experiments yield quite different rotational branching ratios than conventional photoelectron spectroscopy. Merkt and Softley [13] have shown that this is due to effects of rotational autoionization in the ZEKE studies.

Poliakoff and co-workers [17–21] have studied the influence of photon energy on rotational populations using

optical spectroscopy. They measured the fluorescence of N_2^+ and CO^+ , photoionized with synchrotron light. The fluorescence of the transition $B^2\Sigma_u^+ \rightarrow X^2\Sigma_g^+$ for N_2^+ was investigated for photon energies of the ionizing radiation from 20 to 220 eV.

The synchrotron-radiation experiments in the present Letter were performed at the undulator beam line 9.0.1 at the ALS synchrotron facility. This is an extremely high resolution beam line, capable of resolving powers of up to $E/\Delta E = 64\,000$ [4,6]. This beam line is equipped with a spherical grating monochromator with three interchangeable gratings for different energy ranges. A 380 line per mm grating was used for the photon energy range 23 to 45 eV, giving a linewidth of the exciting radiation varying between 2 and 4 meV. At 65 eV, a 925 lines per mm grating was used, with slits set to give a linewidth of around 5 meV. The synchrotron radiation is almost completely linearly polarized. The spectra were recorded at the quasimagic angle $55^\circ \pm 3^\circ$ to the direction of polarization. The uncertainty in angle may introduce a β dependence of the rotational branching ratios, which also may change with photon energy. However, the error can be estimated to be of the order of at most 5%–10%, and will not affect the qualitative result of the present Letter.

The photoelectron spectrometer was a truncated hemispherical analyzer, described elsewhere [7,8]. To reduce the Doppler broadening, the sample gas was introduced as an effusive beam, perpendicular both to the ionizing radiation and the acceptance of the spectrometer. This was vital to be able to resolve any rotational structure, since the Doppler broadening would be 6.4 meV for the X state already at $h\nu = 23$ eV. The beam had almost no cooling effect, so the gas was at room temperature when it was ionized. In the ionizing region, electrodes were used for active potential correction of radiation induced work function drifts, as well as reduction of the plasma potential gradients from the residual ions. The energy resolution in the synchrotron-radiation-excited spectra varied from 4 meV

at 23 eV photon energy up to 10 meV at 65 eV photon energy. One reason for this increase was that although the Doppler broadening was suppressed in the effusive beam, it still increased with the kinetic energy of the photoelectrons. Another resolution degrading effect was fluctuations in the synchrotron-radiation intensity by as much as 50%, with a frequency of about 10 Hz. This caused fast variations of the plasma potential, which the active potential correction setup could not handle. The spectra were recorded using a 50% N₂, 50% Ne mixture. The Ne 2p_{3/2} line at 21.565 eV was recorded simultaneously with the N₂ lines, in order to determine the spectrometer function and to energy calibrate the spectra [22].

Figure 1 shows spectra of the X²Σ_g⁺ state for photon energies of 23, 35, and 45 eV. The strong central peak corresponds to transitions where there is no change in the rotational quantum number *N*, and the surrounding structures are branches where the rotational quantum number changes with Δ*N* = ±2 and Δ*N* = ±4. Only transitions with Δ*N* even are allowed since this is a Σ_g⁺ → Σ_g⁺ transition in a homonuclear diatomic molecule [23]. Transitions with larger changes in rotational quantum number than 4 have too low intensity to show up in the spectrum. The energy resolution decreased with increased photon energy, so the intensity cannot immediately be compared from the peak heights. It is nevertheless obvious that the intensity of the Δ*N* = 0 branch relative to the Δ*N* = ±2 and Δ*N* = ±4 branches has decreased at 35 and 45 eV compared to the 23 eV spectrum. The peak height of the Δ*N* = 0 branch is greater for the 45 eV spectrum than for the 35 eV spectrum. At 45 eV this branch is also broader, so it has a higher relative intensity at 45 eV than at 35 eV. The conclusion is that the relative intensity of the Δ*N* = 0 branch has a minimum between 23 and 45 eV. We have curve fitted the spectra with the model of Xie and Zare [24] to obtain the

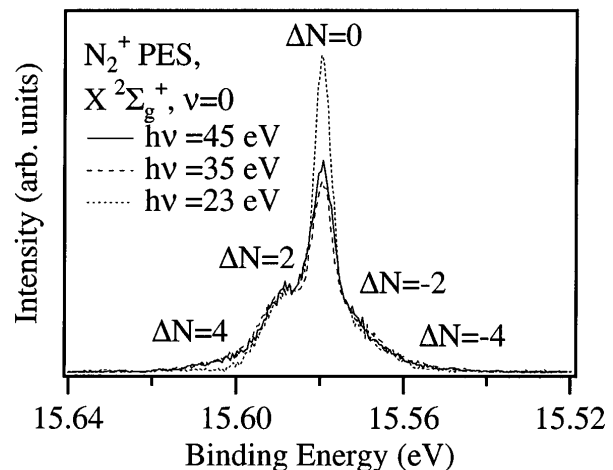


FIG. 1. Synchrotron-radiation-excited spectra of the $\nu = 0$ vibration of the X²Σ_g⁺ state of N₂⁺, recorded at $h\nu = 23$ eV (short-dashed line), at $h\nu = 35$ eV (long-dashed line), and at $h\nu = 45$ eV (solid line). Note that the central feature (the Δ*N* = 0 branch) is stronger in the $h\nu = 23$ eV spectrum than in the $h\nu = 35$ eV and $h\nu = 45$ eV spectra. The Δ*N* = 0 branch of the $h\nu = 45$ eV spectrum has a greater peak height than the $h\nu = 35$ eV spectrum, and is also slightly broader. The relative intensity of the Δ*N* = 0 branch is higher at 45 than at 35 eV, and must go through a minimum between 23 and 45 eV.

squared reduced multipole moment matrix elements of the transition. An example of such a fit is shown in Fig. 2. This model is formally equivalent to the more commonly used BOS model of Buckingham, Orr, and Sichel [25]. As indicated above, the relative intensities of rotational branches vary with photon energy, and hence the multipole moment matrix elements must vary too. In the curve fitting model, the energy positions of the individual rotational states were calculated as

$$E_{b(N,N^+)} = E_{b(0,0)} + B^+N^+(N^+ + 1) - D^+[N^+(N^+ + 1)]^2 - BN(N + 1) + D[N(N + 1)]^2. \quad (1)$$

Literature values were used for the rotational constants [26]. The intensities of the rotational lines were calculated according to the following formula:

$$I(N, N^+) = \frac{3 + (-1)^N}{2} e^{(-\frac{BN(N+1) - D[N(N+1)]^2}{kT})} \sum_k (2N + 1)(2N^+ + 1) \begin{pmatrix} N & k & N^+ \\ 0 & 0 & 0 \end{pmatrix}^2 |\bar{\mu}(k, 0)|^2, \quad (2)$$

with the same notation as in Ref. [24]. The factors $|\bar{\mu}(k, 0)|^2$ are the squared reduced multipole moment matrix elements. Only reduced multipole moments with angular momenta $k \leq 4$ were considered. ($k = 0, 2, 4$ for Δ*N* = 0, $k = 2, 4$ for Δ*N* = ±2, and $k = 4$ for Δ*N* = ±4.) Compared with Ref. [24], a factor of 1/3 has been omitted, since only relative values of $|\bar{\mu}(k, 0)|^2$ can be determined. The factor $[3 + (-1)^N]/2$ is to account for the nuclear spin degeneration of the ground state rotational population in N₂. Each rotational state was broadened with two Gaussians, one due to the Doppler reduced effusive beam which is only spectrometer broad-

ened, and one due to scattered molecules, which is fully Doppler and spectrometer broadened. The ratio between these two contributions was found from the Ne line that was recorded simultaneously.

Plots of the squared reduced multipole moment matrix elements $|\bar{\mu}(2, 0)|^2$ and $|\bar{\mu}(4, 0)|^2$ relative to $|\bar{\mu}(0, 0)|^2$ versus photon energy are displayed in Fig. 3. For some photon energies two spectra were recorded, and this gives an estimate of the statistical scatter of the data. The coupling of the intensity of the rotational branches and the multipole moments make the error estimation very difficult, and we have abstained from giving error limits.

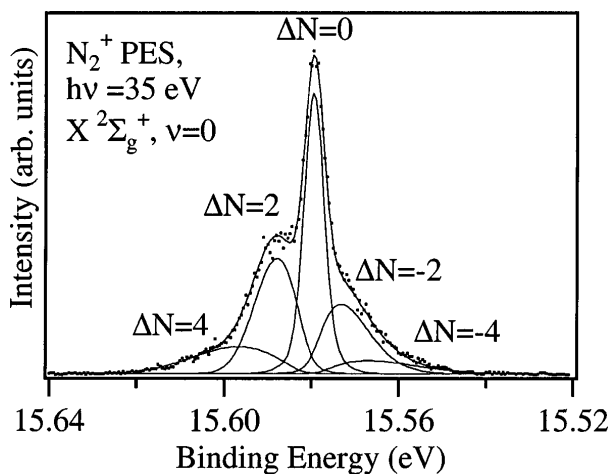


FIG. 2. Experimental (dots) and fitted (solid line) spectra of the $X^2\Sigma_g^+$ state of N_2^+ plotted together. The experimental spectrum was recorded at $h\nu = 35$ eV. The rotational branches of the fit are also shown in the figure.

The $|\bar{\mu}(2,0)|^2$ squared reduced multipole moment matrix element has a maximum relative $|\bar{\mu}(0,0)|^2$ at around 30 eV. Except for at 65 eV, the $|\bar{\mu}(2,0)|^2$ squared multipole moment matrix element is the greatest of the three. The $|\bar{\mu}(4,0)|^2$ squared reduced multipole moment matrix element has a maximum around 35 eV relative to the $|\bar{\mu}(0,0)|^2$ squared reduced multipole moment matrix element.

The X state has a well-known shape resonance [27–29] in the photon energy range that we have studied, and this could well influence the rotational branching ratio of the molecule. Other authors have noticed influences of shape resonances on rotational branching ratios [18,19,30,31]. In particular, Poliakoff *et al.* [19] see an enhancement of large ΔN transitions at low photon energies in the

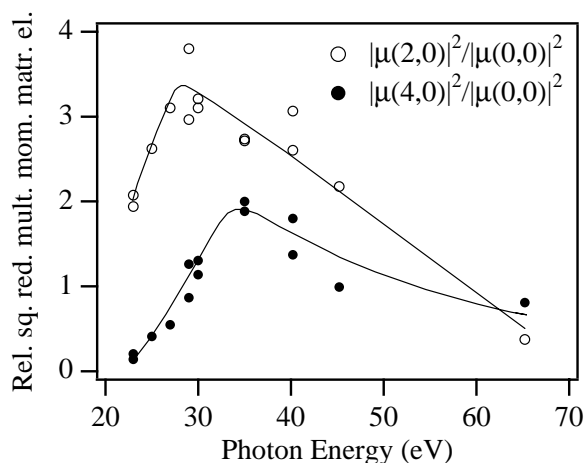


FIG. 3. Relative squared reduced multipole moment matrix elements of the transition $X^1\Sigma_g^+$ ($\nu = 0$) \rightarrow $X^2\Sigma_g^+$ ($\nu = 0$) as a function of photon energy. Unfilled circles $|\bar{\mu}(2,0)|^2/|\bar{\mu}(0,0)|^2$; filled circles $|\bar{\mu}(4,0)|^2/|\bar{\mu}(0,0)|^2$. The lines are intended as guides to the eye.

B state of CO^+ as a result of a $4\sigma \rightarrow k\sigma$ shape resonance. West *et al.* [28] measured strong variations in the $\nu = 1:\nu = 0$ vibrational branching ratio of the X state of N_2^+ between 20 and 40 eV photon energy, with the largest deviations from ordinary Franck-Condon behavior around 35 eV, in agreement with theory [27,29]. Iga *et al.* [32] extended the study of West *et al.* [28] to include the $\nu = 2$ vibration and the angular distribution of the vibrations, with similar results. In an analogous fashion, the $|\bar{\mu}(2,0)|^2$ and $|\bar{\mu}(4,0)|^2$ squared reduced multipole moment matrix elements both have maxima relative the $|\bar{\mu}(0,0)|^2$ squared reduced multipole moment matrix element at around 30–35 eV. Apparently, the σ_u shape resonance influences the rotational population in the $X^2\Sigma_g^+$ ($\nu = 0$) state, favoring larger ΔN transitions around the actual resonance.

In conclusion, very high resolution vacuum ultraviolet photoelectron spectra of the $X^2\Sigma_g^+$ ($\nu = 0$) state in the N_2^+ molecule have been recorded with photon energies ranging from 23 to 65 eV. The resolution of these spectra has been sufficient to observe the rotational line profile of this state. Curve fitting has been used to determine the squared reduced multipole moment matrix elements. These have a clear dependence on photon energy, which can be explained by the $3\sigma_g \rightarrow k\sigma_u$ shape resonance. As seen above, rotationally resolved photoelectron spectra can be a very useful tool in studying the dynamics of molecules, but further investigations, both experimental and theoretical, are needed to gain more insight. A natural extension of the present work would be to study the β parameter of rotational branches or states as a function of photon energy. At present, this would be a difficult experiment to perform with our equipment, since the extremely high-resolution Uppsala spectrometer is not set up for quick changes of angle.

We thank Professor S. Svensson for valuable comments on the manuscript. We want to express our gratitude to Dr. A. Schlachter of the Advanced Light Source, who has been of assistance in both performing the experiment and in the preparation of the manuscript.

- [1] L. Åsbrink, Chem. Phys. Lett. **7**, 549 (1970).
- [2] A. Niehaus and M.W. Ruf, Chem. Phys. Lett. **11**, 55 (1971).
- [3] J.E. Pollard, D.J. Trevor, J.E. Reutt, Y. T. Lee, and D. A. Shirley, Chem. Phys. Lett. **88**, 434 (1982).
- [4] P. Heimann, T. Warwick, M. Howells, W. McKinney, D. Digennaro, B. Gee, D. Yee, and B. Kincaid, Nucl. Instrum. Methods Phys. Res., Sect. A **319**, 106 (1992).
- [5] H. A. Padmore and T. Warwick, J. Synchrotron Radiat. **1**, 27 (1994).
- [6] K. Schulz, G. Kaindl, M. Domke, J.D. Bozek, P. A. Heimann, A. S. Schlachter, and J. M. Rost, Phys. Rev. Lett. **77**, 3086 (1996).
- [7] P. Baltzer, B. Wannberg, and M. Göthe, Rev. Sci. Instrum. **62**, 643 (1991).

- [8] P. Baltzer, L. Karlsson, M. Lundqvist, and B. Wannberg, *Rev. Sci. Instrum.* **64**, 2179 (1993).
 [9] P. Baltzer, L. Karlsson, and B. Wannberg, *Phys. Rev. A* **46**, 315 (1992).
 [10] J.D. Allen, Jr. and F.A. Grimm, *Chem. Phys. Lett.* **66**, 72 (1979).
 [11] Y. Morioka, Y. Hanada, K. Kihara, S. Hara, and M. Nakamura, *J. Phys. B* **18**, 1369 (1985).
 [12] S. Ogata, S. Takahashi, S. Hara, and M. Nakamura, *J. Phys. B* **20**, 3385 (1987).
 [13] F. Merkt and T.P. Softley, *Phys. Rev. A* **46**, 302 (1992).
 [14] W. Kong, D. Rodgers, J.W. Hepburn, K. Wang, and V. McKoy, *J. Chem. Phys.* **99**, 3159 (1993).
 [15] J.W. Hepburn, *J. Chem. Phys.* **107**, 7106 (1997).
 [16] F. Merkt and P.M. Guyon, *J. Chem. Phys.* **99**, 3400 (1993).
 [17] S. Kakar, H.C. Choi, and E.D. Poliakoff, *J. Chem. Phys.* **97**, 6998 (1992).
 [18] H.C. Choi, R.M. Rao, A.G. Mihill, S. Kakar, E.D. Poliakoff, K. Wang, and V. McKoy, *Phys. Rev. Lett.* **72**, 44 (1994).
 [19] E.D. Poliakoff, H.C. Choi, R.M. Rao, A.G. Mihill, S. Kakar, K. Wang, and V. McKoy, *J. Chem. Phys.* **103**, 1773 (1995).
 [20] R.M. Rao, E.D. Poliakoff, K. Wang, and V. McKoy, *J. Chem. Phys.* **104**, 9654 (1996).
 [21] E.D. Poliakoff and R.M. Rao, *J. Electron Spectrosc. Relat. Phenom.* **79**, 361 (1996).
 [22] C.E. Moore, in *Atomic Energy Levels*, edited by C.C. Keiths, Natl. Bur. Stand. (U.S.) Circular No. 467 (U.S. GPO, Washington, DC, 1949).
 [23] J. Xie and R.N. Zare, *J. Chem. Phys.* **93**, 3033 (1990).
 [24] J. Xie and R.N. Zare, *J. Chem. Phys.* **97**, 2891 (1992).
 Equation (2) will, if the $3j$ symbols are explicitly expanded for each ΔN , read like

$$\begin{aligned}
 I(N, N^+ = N) &= \frac{3 + (-1)^N}{2} e^{-\frac{BN(N+1) - D[N(N+1)]^2}{kT}} \\
 &\quad \times \left((2N+1) |\bar{\mu}(0,0)|^2 + \frac{(N+1)N(2N+1)}{(2N+3)(2N-1)} |\bar{\mu}(2,0)|^2 + \frac{9(N+2)(N+1)N(N-1)(2N+1)}{4(2N+5)(2N+3)(2N-1)(2N-3)} |\bar{\mu}(4,0)|^2 \right), \\
 I(N, N^+ = N+2) &= \frac{3 + (-1)^N}{2} e^{-\frac{BN(N+1) - D[N(N+1)]^2}{kT}} \\
 &\quad \times \left(\frac{3(N+2)(N+1)}{2(2N+3)} |\bar{\mu}(2,0)|^2 + \frac{5(N+3)(N+2)(N+1)N}{2(2N+7)(2N+3)(2N-1)} |\bar{\mu}(4,0)|^2 \right), \\
 I(N, N^+ = N-2) &= \frac{3 + (-1)^N}{2} e^{-\frac{BN(N+1) - D[N(N+1)]^2}{kT}} \left(\frac{3N(N-1)}{2(2N-1)} |\bar{\mu}(2,0)|^2 + \frac{5(N+1)N(N-1)(N-2)}{2(2N+3)(2N-1)(2N-5)} |\bar{\mu}(4,0)|^2 \right), \\
 I(N, N^+ = N+4) &= \frac{3 + (-1)^N}{2} e^{-\frac{BN(N+1) - D[N(N+1)]^2}{kT}} \left(\frac{35(N+4)(N+3)(N+2)(N+1)}{8(2N+7)(2N+5)(2N+3)} |\bar{\mu}(4,0)|^2 \right), \\
 I(N, N^+ = N-4) &= \frac{3 + (-1)^N}{2} e^{-\frac{BN(N+1) - D[N(N+1)]^2}{kT}} \left(\frac{35N(N-1)(N-2)(N-3)}{8(2N-1)(2N-3)(2N-5)} |\bar{\mu}(4,0)|^2 \right).
 \end{aligned}$$

- [25] A.D. Buckingham, B.J. Orr, and J.M. Sichel, *Philos. Trans. R. Soc. London A* **268**, 147 (1970).
 [26] K.P. Huber and G. Herzberg, *Molecular Spectra and Molecular Structure IV, Constants of Diatomic Molecules* (Van Nostrand Reinhold, New York, 1979).
 [27] J.L. Dehmer, D. Dill, and S. Wallace, *Phys. Rev. Lett.* **43**, 1005 (1979).
 [28] J.B. West, A.C. Parr, B.E. Cole, D.L. Ederer, R. Stocbauer, and J.L. Dehmer, *J. Phys. B* **13**, L105 (1980).
 [29] R.R. Lucchese and V. McKoy, *J. Phys. B* **14**, L629 (1981).
 [30] E.D. Poliakoff, L.A. Kelly, L.M. Duffy, B. Space, P. Roy, S.H. Southworth, and M.G. White, *Chem. Phys.* **129**, 65 (1989).
 [31] M. Braunstein, V. McKoy, S.N. Dixit, R.G. Tonkyn, and M.G. White, *J. Chem. Phys.* **93**, 5345 (1990).
 [32] I. Iga, A. Svensson, and J.B. West, *J. Phys. B* **22**, 2991 (1989).